Elastic constants and tensile properties of Al_2OC by density functional calculations

R. Yu,[1,*] X. F. Zhang,[1,†] L. C. De Jonghe,[1,2] and R. O. Ritchie[1,2]
[1]*Materials Sciences Division, Lawrence Berkeley National Laboratory, Berkeley, California 94720, USA*
[2]*Department of Materials Science and Engineering, University of California, Berkeley, California 94720, USA*
(Received 19 November 2006; revised manuscript received 17 January 2007; published 26 March 2007)

Al_2OC is a compound that forms as a nanoscale grain-boundary crystalline film in silicon carbide ceramics, and is responsible for imparting high low-temperature toughness and high-temperature creep strength in these materials. The elastic properties and ultimate strengths properties of Al_2OC are determined from first-principles calculations. The crystal structure of Al_2OC was approximated by an optimized model based on the wurtzite structure. The full set of single-crystal elastic stiffness c_{ij} was calculated, from which the polycrystalline elastic constants were obtained by using the Voigt-Reuss-Hill averaging scheme. The tensile properties and the ideal strength in [001] direction of Al_2OC were also computed and compared to those of SiC, where it was found that indeed, Al_2OC is the weaker and more brittle phase, supporting fracture mechanics expectations for SiC containing Al_2OC-type intergranular films.

DOI: 10.1103/PhysRevB.75.104114 PACS number(s): 62.20.Dc, 81.40.Jj, 81.05.Zx

I. INTRODUCTION

The mechanical properties of polycrystalline, brittle materials, such as SiC depend critically on the nature of the intergranular bonding. Specifically, the resistance to crack propagation can be raised dramatically by the presence of nanometer-thick grain-boundary films that are weaker than the surrounding matrix. There are several examples of this where Al_2OC can be an interfacial phase, for example, in composites of SiC and Al_2O_3,[1] and most notably where SiC is sintered with Al, B, and C additives to make ABC-SiC, the toughest SiC ceramic reported to date.[2–6] Since the mechanical characteristics of Al_2OC are unknown (the boundary films are too small, ~1 to 3 nm thick, for direct experimental measurement), it has been difficult to rationalize such unprecedented toughness levels in silicon carbides containing such intergranular Al_2OC-type films. Accordingly, here we follow a computational route to determine elastic and ultimate strength properties of Al_2OC, a wurtzite-type structure, and to ascertain if the properties of Al_2OC conform to fracture mechanics expectations for the toughness of SiC ceramics.

The wurtzite form of aluminum oxycarbide (Al_2OC) is isostructural and isoelectronic with the 2H polymorphs of SiC and AlN. Through alloying with these carbides and nitrides, Al_2OC provides an additional means for controlling their microstructure and properties.[7–12] For example, solid solutions such as AlN-Al_2OC and SiC-AlN-Al_2OC (also called SiCAlON) have been successfully synthesized.[7–12]

In contrast to the well characterized SiC, AlN, and Al_2O_3 compounds, the mechanical properties of Al_2OC are difficult to determine experimentally. This is primarily due to the metastability of Al_2OC at room temperature and, as noted above, the small-scale of Al_2OC as an intergranular, metastable phase. In equilibrium, single phase Al_2OC can only exist above 1715° C; below this temperature it tends to decompose into Al_4O_4C and Al_4C_3.[13,14] At room temperature, the transformation of Al_2OC is kinetically hindered, but can be retained by rapid cooling from the high-temperature processing steps.

In this paper, we approach the problem of determining the experimentally unavailable properties of Al_2OC with first-principles calculations. The full set of single crystal elastic constants, the polycrystalline elastic constants, and the tensile properties were computed, together with the mechanical properties of SiC for comparison.

II. CALCULATION DETAILS

All computations were based on the density functional theory.[15,16] Structural optimization and mechanical properties were calculated using the pseudopotential plane-wave method, as implemented in the ABINIT package.[17] We used norm conserving Troullier-Martins pseudopotentials[18] for the four elements, and a cutoff energy of 70 Ry for the plane-wave expansion. The local density approximation (LDA) exchange-correlation functional of Perdew and Zunger[19] was employed. Integrations over the Brillouin zone were approximated by the special k-points method.[20] The k-point sampling in the Brillouin zone and the plane-wave cutoff energy were tested to ensure that the absolute total energies converged to 3 meV/atom, that the relative total energies between different models converged to 0.3 meV/atom, and that the elastic constants converged to within 2 GPa. During the calculations of the equation of state, the single-crystal elastic constants, and the tensile strength, the relaxations of both the internal structural parameters and the cell shape were included. The structural relaxation was performed until the residual forces and stresses were less than 5×10^{-5} Hartree/Bohr and 5×10^{-7} Hartree/Bohr^3, respectively.

The electronic structures were analyzed with the full-potential linearized augmented plane waves (FLAPW) method.[21] Augmented plane waves plus local orbitals (APW+lo) (Ref. 22) were used for the valence states, while conventional LAPWs were applied to the other states. The total and partial densities of states (DOS) were obtained from the modified tetrahedron method of Blöchl *et al.*[23]

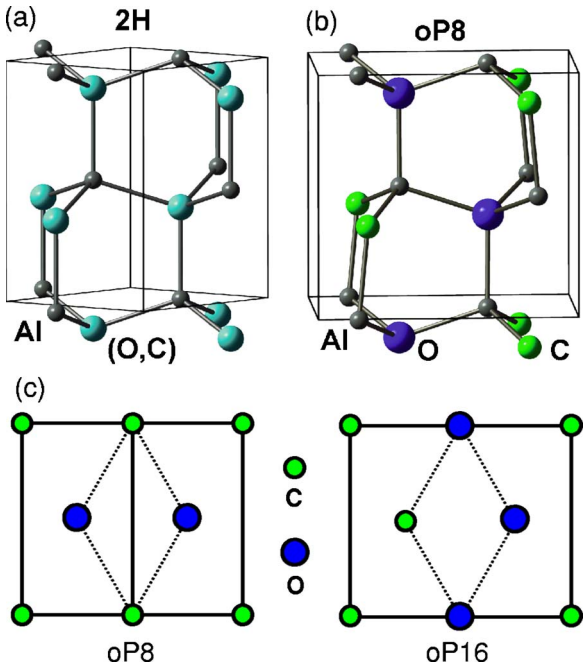

FIG. 1. (Color online) (a) Schematic unit cell of the 2H structure. (b) An ordering model of *oP*8 based on the 2H structure. Each Al atom has two O and two C neighbors, while all neighbors of O and C are Al. (c) The ordering patterns in the (O, C) plane for the models *oP*8 and *oP*16. The solid and dotted lines outline the orthorhombic supercells and the corresponding disordered 2H unit cell, respectively. For the *hP*4 structure (not shown here), the ordering occurs along the *c* direction (normal to the paper).

III. RESULTS AND DISCUSSIONS

A. Crystal structure and energetics

At high temperatures, Al_2OC [or written as Al (O, C) to show the similarity with AlN and SiC] has a hexagonal 2H-wurtzite structure in which O and C atoms occupy the nonmetal positions randomly [Fig. 1(a)].[7,13] Rapid cooling to room temperature results in retention of a metastable Al_2OC, in which the short-range O and C ordering complicates the experimental determination of the crystal structure.[24,25] Here, we use supercell models, in which O and C atoms occupy ordered positions, to approximate the wurtzite-type Al_2OC phase. It should be noted that we say the wurtzite-type Al_2OC only in the statistical meaning. Microscopically, Al_2OC would never exist in the wurtzite-type structure because the local ordering of O and C unavoidably breaks the symmetry of the wurtzite structure. It is, however, reasonable to assume that if a model structure and the actual material have similar atomic coordination and similar structural parameters, they would have similar mechanical properties.

Three ordered structural models are considered here. In the first model, the nonmetal planes are composed of both O and C atoms [Fig. 1(b)]; each Al atom has two O and two C neighbors, while all neighbors of O and C are Al, so that each Al-O-C tetrahedron is composed of two O and two C at the corners and one Al in the center. This type of ordering reduces the symmetry from hexagonal to orthorhombic, i.e., the space group changes from $P6_3mc$ of the wurtzite structure to $Pmc2_1$. This model is referred to as *oP*8 after its Pearson symbol. In the second model, the nonmetal planes composed of either O or C atoms stack alternatively along the *c*-axis direction. In each unit cell, one Al atom has one O and three C neighbors, and another Al atom has three O and one C neighbors. This type of ordering reduces the space group to $P3m1$. This model structure is referred to as *hP*4. The third model is similar to *oP*8 in terms of the nearest neighbors, but the ordering pattern in the (O, C) plane is different [Fig. 1(c)]. This model has a space group of $Pna2_1$ and will be referred to as *oP*16.

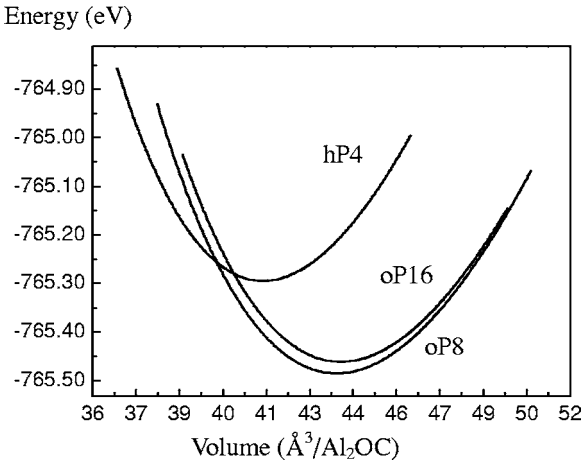

FIG. 2. The total energies of the Al_2OC model structures as a function of volume. *oP*8 has the lowest energy at its equilibrium volume, while *hP*4 is more stable at high pressures (small volumes). The curves were fitted using the Vinet equation of state.

By fitting the total energy as a function of the unit cell volume to the Vinet equation of state,[26] which is one of the more accurate formulations for equations of state,[27] the minimum energies and the equilibrium volumes of the three Al_2OC models were obtained, as shown in Fig. 2. The optimized lattice parameters, total energies, bulk moduli, and the atomic coordinates of the three Al_2OC models are listed in Table I and Table II, respectively. At equilibrium, the total energies of *hP*4 and *oP*16 are higher than *oP*8 by 187 meV and 23 meV per Al_2OC, respectively, implying that *hP*4 and *oP*16 are unstable relative to *oP*8 at ambient pressure. More importantly, *oP*8 has similar atomic coordination and structural parameters to those experimentally measured for Al_2OC. Therefore, for more detailed calculations, we focused on the *oP*8 model. Specifically, the electronic structure, elastic constants, and ideal tensile strength were computed. For comparison, some properties of the well-characterized SiC were also calculated.

It is interesting to note that the coordination relationship of *hP*4 changed after the relaxation. The new structure has a space group of $P\bar{6}m2$, and the Al atoms are coplanar with C or O in the (0001) planes. Model *hP*4 has less equilibrium volume than *oP*8, and becomes more stable at high pressures. By comparing the enthalpy ($H=E+pV$, E is the internal energy, p is the pressure, and V is the volume) of *hP*4 and *oP*8, the transition pressure was determined to be 13 GPa.

TABLE I. Lattice parameters, total energies, and bulk moduli of Al_2OC. *oP*8 has the lowest energy and is used as a reference for the total energy. The experimental values (Refs. 13 and 28) are given in parentheses. For *oP*8 and *oP*16, the experimental values are scaled to the corresponding supercells. The results for two SiC polytypes (the wurtzite structured 2H-SiC and the zinc-blende structured 3C-SiC) are also listed for comparison.

Models	*a* (Å)	*b* (Å)	*c* (Å)	Energy (eV/formula)	Bulk modulus (GPa)
*oP*8	3.273 (3.17)	5.330 (5.49)	5.030 (5.06)	0	163
*oP*16	5.889 (5.49)	6.231 (6.34)	5.057 (5.06)	0.023	165
*hP*4	3.435 (3.17)		4.048 (5.06)	0.187	186
3C-SiC	4.331 (4.360)			0	228
2H-SiC	3.059 (3.076)		5.017 (5.048)	0.014	229

B. Electronic structure

Figures 3(a) and 3(b) show the total density of states and the valence charge density of Al_2OC, respectively. Al_2OC is an insulator with a band gap of about 3 eV. We note that the LDA calculations generally underestimate the band gap, but more accurate calculations of this gap (for example, by the GW approximation) were beyond the scope of the present study. The valence bands are mainly composed of the C 2*s*, O 2*p*, and C 2*p* states. Due to the larger electronegativity of O compared to C, the O states have lower energy, and are more localized, as evidenced by the narrower band. The partial DOS of Al is very low in the valence bands because of the charge transfer from Al to O and C. The charge transfer can be seen directly from the charge density map shown in Fig. 3(b), in which the valence charge density is much lower around Al than around O and C, indicating the ionic character of Al_2OC.

TABLE II. Atomic coordinates of Al_2OC. (No experimental values are available.)

Space group		Wyckoff letter	*x*	*y*	*z*
*oP*8 ($Pmc2_1$)	Al(1)	2*b*	0.5	0.6687	0.9960
	Al(2)	2*a*	0	0.1558	0.9968
	O	2*b*	0.5	0.6706	0.3771
	C	2*a*	0	0.1896	0.3789
*hP*4 ($P\bar{6}m2$)	Al(1)	1*a*	0	0	0
	Al(2)	1*d*	1/3	2/3	0.5
	O	1*b*	0	0	0.5
	C	1*c*	1/3	2/3	0
*oP*16 ($Pna2_1$)	Al(1)	4*a*	0.0765	0.6337	0.9881
	Al(2)	4*a*	0.0818	0.1182	0.9919
	O	4*a*	0.0801	0.6239	0.3700
	C	4*a*	0.1020	0.1232	0.3720

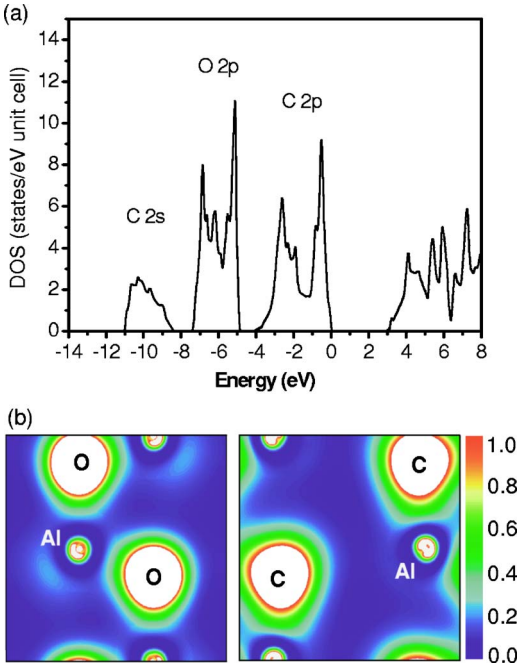

FIG. 3. (Color online) (a) Density of states, and (b) valence charge density (in electron/Å^3) of Al_2OC (*oP*8). The Fermi level lies at the energy zero in the DOS plot.

C. Mechanical properties

While the bulk modulus of a material can be readily calculated from the equation of state, the full set single-crystal elastic constants are needed to obtain the shear modulus. Here we extract the elastic constant from fitting the calculated stresses to applied strains. The nine single-crystal elastic constants of Al_2OC are listed in Table III. The polycrystalline elastic constants were calculated from the single-crystal elastic constants using the Voigt-Reuss-Hill averaging scheme.[29] Note that the bulk modulus obtained from the equation-of-state fitting and that from the Voigt-Reuss-Hill averaging can be used as a check of the precision of the calculations. In the present case, the two values are almost identical (163 GPa vs 164 GPa). The eigenvalues of the elastic stiffness matrix are 71, 93, 98, 177, 183, 503, indicating that the matrix is positive-definite, and that the crystal is mechanically stable, although energetically metastable at low temperatures. For comparison, we also calculated the bulk moduli of two polytypes of SiC, which are 229 GPa and 228 GPa, respectively. They are in good agreement with the experimental value of 225 GPa.[30]

To calculate the ideal tensile strengths for Al_2OC and 2H-SiC, the crystals were subjected through a series of incremental strains, with the corresponding stresses calculated with the Hellmann-Feynman theorem. Poisson's contractions were applied until the stress components normal to the applied strain were less than 0.1 GPa. Atomic coordinates were also relaxed by this procedure. Based on the widely adopted assumption[31] that other instabilities (such as soft phonon

TABLE III. The single-crystal elastic stiffness constants c_{ij} of Al_2OC ($oP8$). The polycrystalline bulk moduli (B), shear moduli (G), Young's moduli (E), and Poisson's ratio ν were obtained using the Voigt-Reuss-Hill averaging scheme. All the elastic constants are in GPa except for the dimensionless ν.

c_{11}	c_{12}	c_{13}	c_{22}	c_{23}	c_{33}	c_{44}	c_{55}	c_{66}	B	G	E	ν
331	116	113	267	84	265	71	93	98	164	87	225	0.27

modes[32]) have no effect at stresses lower than the peak stress, the peak stress in the predicted stress-strain curve was taken to correspond to the ideal tensile strength.

The computed stress-strain curves, shown in Fig. 4(a) for Al_2OC and 2H-SiC along the [001] direction, provided the basis for the calculation of the Young's moduli and the ideal strengths, which are listed in Table IV. For comparison, the ideal tensile strength of 50.0 GPa was computed for 2HSiC, which is close to values quoted in the literature based on experimental measurement (53.4 GPa) (Ref. 33) and other theoretical calculation (50.4 GPa).[34] Because the [001] tensile direction is the elastically stiffest one for SiC, the calculated Young's modulus of 534 GPa is greater than the experimentally measured value of 448 GPa for hot-pressed, polycrystalline SiC. For Al_2OC, the calculated Young's modulus and the strain at the peak stress were found to be 246 GPa and 10%, respectively, giving an ideal tensile strength of 22.5 GPa. As for SiC, Young's modulus in the [001] direction of Al_2OC is also larger than the polycrystalline value (225 GPa).

Figure 4(b) shows the bond lengths for Al_2OC under [001] tension. As described above, all four neighbors of O and C are Al for Al_2OC. Among the four Al-anion bonds in each tetrahedron, one is parallel to the [001] direction, and the other three are at about 110° to the [001] direction. There are two tetrahedra in each unit cell, one with one Al-O bond parallel to the [001] direction, the other with one Al-C bond parallel to the [001] direction. Since the calculated bond lengths of the three Al-anion bonds that are not parallel to the [001] axis are not equal, only an arithmetic average is shown in Fig. 4(b) for clarity. The calculations showed that the bonds along the tensile direction were elongated, whereas the other bonds were nearly unchanged under the [001] tension. The change in bond lengths for Al-O is more prominent than for Al-C. At strains larger than 10%, the Al-O bond is stretched to rupture. Thus, the Al-O bond is weaker than the Al-C bond in Al_2OC. This is somewhat surprising considering that Al-O bonds are generally thought to be strong, as manifested by the high hardness of Al_2O_3. However, we note that Al and O in Al_2O_3 form octahedra, instead of tetrahedra. This means that the tetrahedral coordination of Al by O in Al_2OC is not the preferred configuration, resulting in the weaker bonding interaction between Al and O. In contrast, the Al and C are in a tetrahedra configuration in Al_4C_3, suggesting that the tetrahedral coordination in Al_2OC is a favorable environment for the Al and C atoms, forming strong bonds.

TABLE IV. The calculated Young's moduli E, ideal tensile strengths σ_{id}, and the peak strains along the [001] direction of Al_2OC ($oP8$) and 2H-SiC.

	E (GPa)	σ_{id} (GPa)	Peak strain
Al_2OC	246	22.5	10%
2H-SiC	534	50.0	16%

IV. CONCLUSIONS

The mechanical properties and electronic structure of Al_2OC, a nanoscale intergranular phase found in SiC ceramics or a metastable component stabilized in wurtzite composites, have been investigated using first-principles calculations based on an optimized structure model. The full set of single-crystal elastic constants, the polycrystalline elastic constants, and the tensile properties along the [001] direction have been

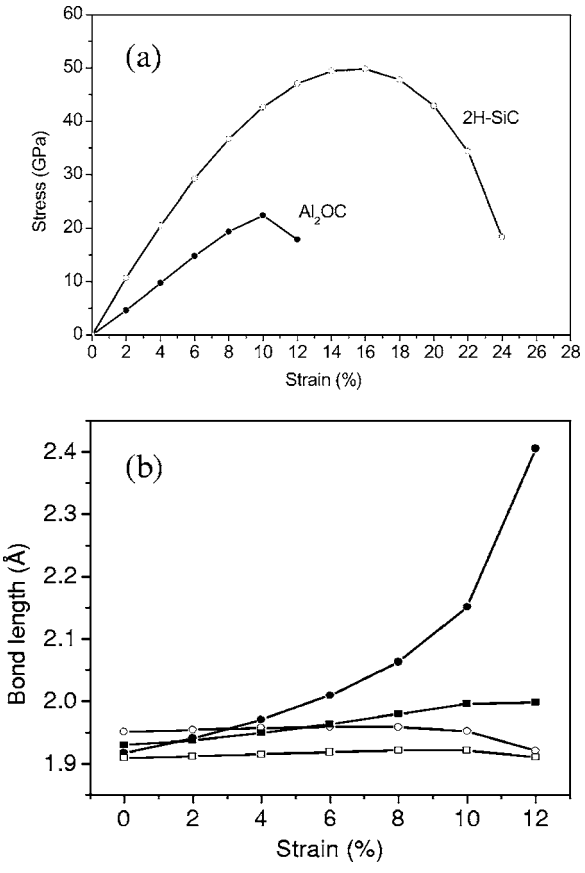

FIG. 4. (a) Computed stress-strain curves for Al_2OC ($oP8$) and 2H-SiC along the [001] direction; (b) Al-O bond length (circles) and Al-C bond length (squares) in Al_2OC under the [001] tension. The solid and open symbols denote the bonds parallel and oblique to the [001] tensile direction, respectively.

calculated. Generally speaking, the strength of Al_2OC is about one-half that of SiC. As the presence of Al_2OC boundary films in SiC is known to impart high toughness in SiC by inducing intergranular fracture, these calculations provide the conformation that cracks in these ceramics should deflect along the grain boundaries within the low strength Al_2OC-type intergranular films. While Al_2OC would be unsuitable as a single-phase strong solid, it provides a practical and controllable means for modifying the mechanical properties of known materials, e.g., as an alloying component in AlN (Refs. 1–6) or an additive to SiC.[7–9]

ACKNOWLEDGMENTS

This work was supported by the Director, Office of Science, Office of Basic Energy Sciences, Division of Materials Sciences and Engineering of the U.S. Department of Energy under Contract No. DE-AC02-05CH11231. This research used resources of the National Energy Research Scientific Computing Center (NERSC), which is supported by the Office of Science of the U.S. Department of Energy under Contract No. DE-AC03-76SF00098. One of the authors (R.Y.) thanks Andrew Canning for assistance with NERSC.

*Electronic address: ryu@lbl.gov
†Present address: Hitachi High Technologies America, Inc., Pleasanton, California 94588.

[1] G. Urretavizcaya, J. M. P. Lopez, and A. L. Cavalieri, J. Eur. Ceram. Soc. **17**, 1555 (1997).
[2] J. J. Cao, W. J. MoberlyChan, L. C. De Jonghe, C. J. Gilbert, and R. O. Ritchie, J. Am. Ceram. Soc. **79**, 461 (1996).
[3] C. J. Gilbert, J. Cao, W. J. MoberlyChan, L. C. De Jonghe, and R. O. Ritchie, Acta Mater. **44**, 3199 (1996).
[4] X. F. Zhang, M. E. Sixta, and L. C. De Jonghe, J. Am. Ceram. Soc. **83**, 2813 (2000).
[5] R. Yuan, J. J. Kruzic, X. F. Zhang, L. C. De Jonghe, and R. O. Ritchie, Acta Mater. **51**, 6477 (2003).
[6] X. F. Zhang and L. C. De Jonghe, J. Mater. Res. **19**, 2510 (2004).
[7] I. B. Cutler, P. D. Miller, W. Rafaniello, H. K. Park, D. P. Thompson, and K. H. Jack, Nature (London) **275**, 434 (1978).
[8] J. M. Lihrmann, J. Tirlocq, P. Descamps, and F. Cambier, J. Eur. Ceram. Soc. **19**, 2781 (1999).
[9] L. Huang, A. C. Hurford, R. A. Cutler, and A. V. Virkar, J. Mater. Sci. **21**, 1448 (1986).
[10] S. Y. Kuo and A. V. Virkar, J. Am. Ceram. Soc. **72**, 540 (1989).
[11] J. Chen, Q. Tian, and A. V. Virkar, J. Am. Ceram. Soc. **76**, 2419 (1993).
[12] Q. Tian and A. V. Virkar, J. Am. Ceram. Soc. **79**, 2168 (1996).
[13] J. M. Lihrmann, T. Zambetakis, and M. Daire, J. Am. Ceram. Soc. **72**, 1704 (1989).
[14] C. Qiu and R. Metselaar, J. Am. Ceram. Soc. **80**, 2013 (1997).
[15] P. Hohenberg and W. Kohn, Phys. Rev. **136**, B864 (1964).
[16] W. Kohn and L. J. Sham, Phys. Rev. **140**, A1133 (1965).
[17] X. Gonze *et al.*, Comput. Mater. Sci. **25**, 478 (2002).
[18] N. Troullier and J. L. Martins, Phys. Rev. B **43**, 1993 (1991).
[19] J. P. Perdew and A. Zunger, Phys. Rev. B **23**, 5048 (1981).
[20] H. J. Monkhorst and J. D. Pack, Phys. Rev. B **13**, 5188 (1976).
[21] P. Blaha, K. Schwarz, G. K. H. Madsen, D. Kvasnicka, and J. Luitz, WIEN2K, An augmented plane wave + local orbitals program for calculating crystal properties, Technical Universität Wien, Austria, 2001.
[22] E. Sjöstedt, L. Nordström, and D. J. Singh, Solid State Commun. **114**, 15 (2000).
[23] P. E. Blöchl, O. Jepsen, and O. K. Andersen, Phys. Rev. B **49**, 16223 (1994).
[24] E. L. Amma and G. A. Jeffrey, J. Chem. Phys. **34**, 252 (1961).
[25] G. A. Jeffrey and V. Y. Wu, Acta Crystallogr. **20**, 538 (1966).
[26] P. Vinet, J. Ferrante, J. H. Rose, and J. R. Smith, J. Geophys. Res. **92**, 9319 (1987).
[27] R. E. Cohen, O. Gülseren, and R. J. Hemley, Am. Mineral. **85**, 338 (2000).
[28] W. Martienssen and H. Warlimont, *Springer Handbook of Condensed Matter and Materials Data* (Spinger, Berlin, 2005).
[29] R. Hill, Proc. Phys. Soc. London **65**, 349 (1952).
[30] R. D. Carnahan, J. Am. Ceram. Soc. **51**, 223 (1968).
[31] See, e.g., a review by M. Šob, M. Friák, D. Legut, J. Fialac, and V. Vitek, Mater. Sci. Eng., A **387-389**, 148 (2004).
[32] D. M. Clatterbuck, C. R. Krenn, M. L. Cohen, and J. W. Morris, Phys. Rev. Lett. **91**, 135501 (2003).
[33] E. W. Wong, P. E. Sheehan, and C. M. Lieber, Science **277**, 1971 (1997).
[34] W. Li and T. Wang, Phys. Rev. B **59**, 3993 (1999).